Vol. 23, No. 3(2024) IA24290
Revista Mexicana de Ingeniería Química

Evaluation of the biodegradation, mechanical and barrier properties of extruded corn starch/*Agave tequilana* fiber biocomposites as an alternative to packaging and single-use plastics

Evaluación de la biodegradación, propiedades mecánicas y de barrera de biocompositos extruidos de almidón de maíz/fibras de *Agave tequilana* como una alternativa para empaques y plásticos de un solo uso

M.A. Iniestra-Galindo[1], F. Rodríguez-González[2], J.A. Mendoza-Pérez[3], E.F. Medina-Bañuelos[1], B.M. Marín-Santibáñez [1]*

[1]*Instituto Politécnico Nacional, Escuela Superior de Ingeniería Química e Industrias Extractivas, U.P.A.L.M. C.P. 07738, Col. Lindavista, Alc. Gustavo A. Madero, Ciudad de México, México.*

[2]*Instituto Politécnico Nacional, Departamento de Biotecnología, Centro de Desarrollo de Productos Bióticos, Km 6 Carretera Yautepec-Jojutla, Calle CEPROBI 8, Col. San Isidro. C.P. 62731. Yautepec, Morelos, México.*

[3]*Instituto Politécnico Nacional, Departamento de Ingeniería en Sistemas Ambientales, Escuela Nacional de Ciencias Biológicas, U.P.A.L.M. C.P. 07738, Col. Lindavista, Alc. Gustavo A. Madero, Ciudad de México, México.*

Received: March 8, 2024; Accepted: May 21, 2024

Abstract

In this work, we investigated the mechanical and water-vapor barrier properties, as well as the water solubility and biodegradability of biocomposites obtained by continuous extrusion made up of thermoplastic corn starch (TPS) reinforced with 1, 3, and 8 wt.% of /*Agave tequilana* fibers as an alternative to replace polymer packaging and single-use plastics. We show that increasing the content of *Agave* fibers in biocomposites up to 8 wt.% improves the elastic modulus by 136%, while water-vapor permeability and water solubility decrease by 29% and 17%, respectively. It is also shown that biocomposites are biodegradable in the soil since TPS/*Agave tequilana* fiber sheets underwent the stages of deterioration, fragmentation, and assimilation, which are characteristics of the biodegradation process. Photographic records show that sheets lose their physical integrity over time due to the biodegradation of starch (matrix). The results suggest that biocomposites of thermoplastic corn starch reinforced with *Agave* fibers possess suitable mechanical and physicochemical properties to be used as an alternative to produce biodegradable plastic materials that can replace packaging and single-use synthetic plastics.

Keywords: *Agave tequilana* fibers, corn starch, continuous extrusion, biocomposites, biodegradation.

Resumen

En este trabajo, investigamos las propiedades mecánicas y de barrera al vapor de agua, así como la solubilidad en agua y la biodegradabilidad de biocompositos obtenidos por extrusión continua compuestos por almidón de maíz termoplástico (TPS) reforzado con 1, 3 y 8 %p/p de fibras de *Agave tequilana* Weber variedad azul como alternativa para sustituir envases polímericos y plásticos de un solo uso. Mostramos que aumentar el contenido de fibras de agave en los biocompositos hasta un 8 %p/p mejora el módulo elástico en un 136%, mientras que la permeabilidad al vapor de agua y la solubilidad en agua disminuyen en un 29% y 17%, respectivamente. También se demuestra que los biocompositos son biodegradables en el suelo ya que las láminas de TPS/fibras de *Agave tequilana* pasaron por las etapas de deterioro, fragmentación y asimilación, características del proceso de biodegradación. Los registros fotográficos muestran que las láminas pierden su integridad física con el tiempo debido a la biodegradación del almidón (matriz). Los resultados sugieren que los biocompositos de almidón de maíz termoplástico reforzado con fibras de *Agave* poseen propiedades mecánicas y fisicoquímicas adecuadas para ser utilizados como una alternativa para producir materiales plásticos biodegradables que puedan reemplazar empaques y plásticos sintéticos de un solo uso.

Palabras clave: Fibras de *Agave tequilana*, almidón de maíz, extrusión continua, biocompositos, biodegradación.

* *Corresponding author. E-mail*: bmarin@ipn.mx;
https://doi.org/10.24275/rmiq/IA24290
ISSN:1665-2738, *issn-e*: 2395-8472

1 Introduction

The durability of synthetic polymers has emerged as a severe worldwide pollution problem due to the long time required for degradation once they are finally discarded. This is mainly the case with packaging polymers and single-use plastics, which are used massively but have a very short useful life and are not easy to recycle. This problem has led different countries to impose regulations on the distribution of products that use synthetic plastic materials for packaging (Filiciotto *et al*., 2021). As a result, starch-based bioplastics are a promising substitute for single-use plastics and synthetic polymers for packaging (Cheng *et al*., 2021; Filiciotto *et al*., 2021; García-Guzman *et al*., 2022; Jiang *et al*., 2020; Surendren *et al*., 2022), among other applications.

Starch-based materials are a cost-effective and fully degradable option that can be used to create films and some profiles. However, the processability of starch requires the elimination of its crystalline structure to form an amorphous thermoplastic material. This may be attained by heating the starch in the presence of a large quantity of water or by imposing mechanical work, i.e., extruding the starch with plasticizers with conventional polymer processing equipment (Alanis-López *et al*., 2011; Cheng *et al*., 2021; do Val Siqueira *et al*., 2021). Plasticizers help to form a material known as thermoplastic starch (TPS) by reducing the intermolecular forces and increasing biopolymer chain mobility.

On the other hand, some limitations to the massive use of starch-based plastic materials are their poor resistance to water and reduced mechanical properties as compared to synthetic polymers (Alanis-López *et al*., 2011; do Val Siqueira *et al*., 2021). The mechanical and barrier properties of starch-based products are typically modified by using plasticizers (Cheng *et al*., 2021; do Val Siqueira *et al*., 2021; García-Guzman *et al*., 2022; Mohanty *et al*., 2018; Samir *et al*., 2022; Surendren *et al*., 2022), blending them with synthetic polymers (Biagiotti *et al*., 2004; García-Guzman *et al*., 2022; Surendren *et al*., 2022; Tabasum *et al*., 2019) or adding synthetic or natural particles to produce a biocomposite. Biocomposites are obtained by reinforcing starch-based materials with natural particles like fibers such as sisal, coconut, jute, and *Agave tequilana*, which have been used to reinforce thermoplastic materials made of corn starches (Aranda-García *et al*., 2015; Biagiotti *et al*., 2004; Fitch-Vargas *et al*., 2023; Ji *et al*., 2021; Józó *et al*., 2022; Maya *et al*., 2008; Mohanty *et al*., 2018; Rosa *et al*. 2009). The objective of reinforcing the TPS matrices with fibers is to enhance the interaction between matrix and fibers, which in turn improves the mechanical and barrier properties without affecting biodegradability. It is important to point out that both matrix and fibers should have similar hydrophilic properties to ensure optimum interaction.

Biodegradation is the process of breaking down materials with the help of microorganisms, mainly bacteria, fungi, or enzymes. When the microorganisms interact with biocomposites, the degradation occurs through an enzymatic process that breaks them down into compounds with lower molecular weights. Therefore, the long-term thermal stability and biodegradability of biocomposites are crucial for the safety and reliability of these materials. These properties can be evaluated by controlled exposure to high temperatures or microorganisms. Biocomposites made from starch and agro-industrial waste are entirely biodegradable and compostable. These materials do not cause any harm to the environment when disposed of after their useful life. In recent years, the use of degradable biocomposites has significantly increased in different fields, such as the automotive industry (Wazeer *et al*., 2023), packaging and single-use bioplastics (Cheng *et al*., 2021; Folino *et al*., 2020; García-Guzman *et al*., 2022; Idris *et al*., 2023; Jiang *et al*., 2020; Surendren *et al*., 2022), to name a few. Therefore, the manufacture of biocomposites using starches as matrix materials and fibers derived from agricultural residues as reinforcement is an eco-friendly and promising alternative to single-use plastics.

The water solubility (WS) of neat and reinforced TPS sheets plays a significant role in the production of these biocomposites, along with thermal stability and biodegradability. WS is evaluated by considering the remaining dry matter of the sample after immersion or solubilization in water for a specific time (Escobar *et al*., 2009). Depending on the percentage of WS, the final use of the specimen may be established. Some research has focused on biofilms as edible packaging, where an improved solubility is desired (dos Reis *et al*., 2014). However, when the materials are expected to be used in the manufacturing of single-use bioplastics and packaging, decreasing WS is of concern. Thus, in this work, we investigate the physicochemical properties of extruded thermoplastic corn starch/*Agave tequilana* bagasse fiber (AFs) biocomposites as an alternative to packaging and single-use plastics. The TPS/AFs biocomposites were evaluated for mechanical resistance in uniaxial tension, water vapor permeability, water solubility, and biodegradability according to ASTM test methods. The fibers used in this work were obtained from bagasse of *Agave tequilana* Weber blue variety, which is considered a waste of an inulin and fructans extraction process (López *et al*., 2003).

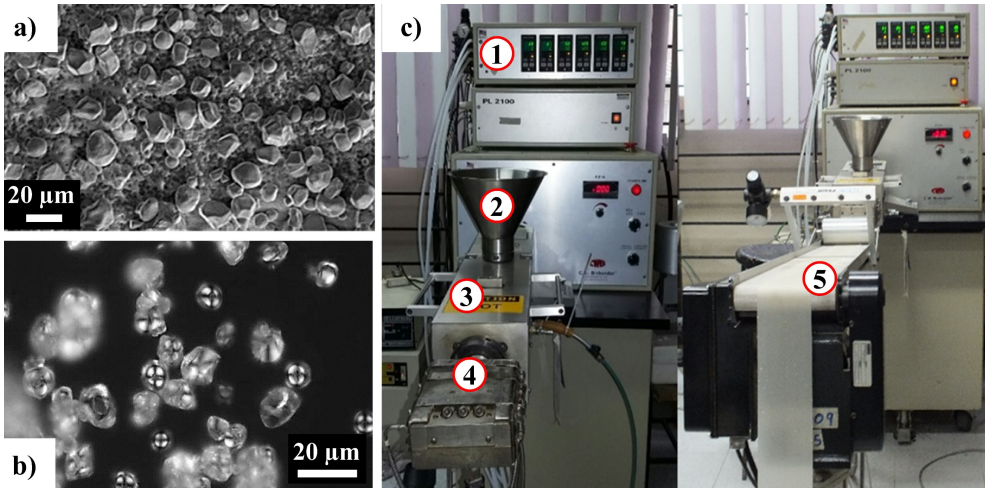

Figure 1. (a) SEM and (b) Optical images of native corn starch granules showing the polyhedral shape and the Maltese cross in a polarized light field. (c) Extrusion system (PL2100, C.W. Brabender®) to obtain TPS sheets with different contents of AFs: 1) Speed and temperature control console, 2) Feed hopper, 3) Twin-screw extruder (C.W. Brabender®), 4) Die for obtaining sheets of variable thickness, 5) Conveyor belt for collecting the sheets.

2 Materials and methods

2.1 *Materials*

Native corn starch (Starch Globe AA, Ingredion) was used as raw material. According to the supplier, this starch contains 22.7% amylose, 77.3% amylopectin, and 12% moisture by weight. The shape and average granular size of native starch granules were analyzed using scanning electron microscopy (SEM, EVO® LS10 Carl ZEISS) and optical microscopy (Eclipse LV100D, Nikon) using a 12.6-megapixel high-definition CCD color camera (DXM1200C, Nikon). SEM and optical images were analyzed with the NIS-Elements software (Basic Research 3.0, Nikon). First, in Figure 1a, the SEM micrograph evinces that the largest granules have a polyhedral shape, while the smallest are spheroidal. The average size of the smallest is 8.14 μm, which is consistent with values reported for corn starch in previous studies (Bertoft, 2017; Cornejo-Ramírez *et al*., 2018). Second, Figure 1b reveals the semi-crystallinity of corn starch granules in a polarized light field by Maltese crosses, which are formed due to the ordered domains of the amylopectin chains (Bertoft, 2017).

On the other hand, *Agave* fibers (AFs) were obtained from the bagasse of the pineapple of ten-year-old *Agave tequilana* Weber blue variety. The bagasse was a waste of the inulin extraction process (López *et al*., 2003), which was dried in the sun and ground in a plastic mill to obtain the AFs. The milled AFs were then passed through sieves of 20 and 70 meshes to attain a specific size distribution. The diameter and length of the AFs were measured using optical microscopy with the NIS element software. The weight-average diameter and length were calculated as D_w=188±46 μm and L_w=3078±899 μm, respectively, which results in an average aspect ratio of $r_w=L_w/D_w$=16.4. The densities of AFs and native corn starch were determined at 25±0.2 °C using a Hubbard pycnometer of 25 mL (Kimax® Kimble Chase) and a general-purpose standard oil (CANNON S60, 859.5 kg/m^3 at 25 °C). Dried and pre-weighed samples of AFs were placed in the pycnometer, which was filled with the standard oil. The masses of the pycnometer filled with standard oil and solid samples, as well as the pycnometer filled only with the standard oil, were registered. From this, the calculated densities of AFs and native corn starch were 1037 kg/m^3 and 864 kg/m^3, respectively, which agree with those reported for other natural fibers (Biagiotti *et al*., 2004) and corn starches (Bertoft, 2017; Cornejo-Ramírez *et al*., 2018).

Regarding solvents and chemicals used in this work, distilled and bi-distilled water were purchased from Reactivos Química Meyer (Química Suastes, S.A. de C.V.), as well as sodium bromide (NaBr) and potassium nitrate (KNO_3), both of ACS reagent grade. USP-grade glycerol was purchased from Droguería Cosmopolita, while the Calcium chloride ($CaCl_2$) and silica gel desiccants were obtained from Sigma-Aldrich.

2.2 *Methods*

2.2.1 *Preparation and extrusion of TPS sheets*

The TPS sheets were prepared without or with AFs by mixing bi-distilled water and glycerol at 80±1 °C. The contents of glycerol and bi-distilled water used in this work were previously reported by Alanís-López *et al*. (2011).

Table 1. Composition of blends to obtain thermoplastic corn starch.

Component	Content (wt.%)		
AFs	8	3	1
Corn starch	55.2	58.2	59.4
Glycerol	27.6	29.1	29.7
Water	9.2	9.7	9.9

The heated mix was slowly incorporated into starch powder at 107 rpm for 30 minutes in a planetary blender (A200, Hobart). Then, the blend homogenization was made at 198 rpm for 30 minutes. The weight concentration of AFs added to corn starch blends are reported in Table 1 and cover the semiconcentrated ($r_w^{-1}<\varphi<r_w^{-2}$, $0.037<\varphi<6.12$ v/v%) and concentrated regimes ($\varphi>6.12$ v/v%). As a qualitative result, the color of the blends changed from almost white (0 wt.% AFs) to light yellow (1 and 3 wt.% AFs) and brown (8 wt.% AFs).

A critical issue for the extrusion of the corn starch and plasticizer blends is their conditioning (Alanis-López *et al*., 2011), which allows the diffusion of glycerol and water into the starch granules for better processability. In this work, the blends were stored in sealed plastic containers for three days before extrusion. TPS sheets were obtained by processing corn starch blends, with and without AFs, in a counter-rotating conical twin-screw extruder (C.W. Brabender®) with three heating zones and an adjustable ribbon die assembly of 0.0762 m wide. The die thickness was set at 800 μm using steel feeler gauge blades (Starrett). This processing equipment has been widely used to prepare food pastes (Castro-Montoya *et al.*, 2024). The extrusion temperature profile was 80, 90, and 98 °C in the heating zones of the extruder and 95 °C in the die head (see Figure 1c). The neat and reinforced TPS sheets were extruded at a constant screw speed of 20 rpm while the torque was continuously monitored during extrusion. The extruded sheets were collected with a conveyor belt (C.W. Brabender®), as shown in Figure 1c, which allows the cooling of sheets under atmospheric conditions.

2.2.2 *Mechanical properties*

Tensile tests of neat and reinforced TPS sheets with AFs were carried out according to the ASTM D638-22 test method using dumbbell shape specimens and a tensile machine (Com-Ten Industries) with an S-beam load cell (9.07 kg-f) and an accuracy of ±0.5%. Experiments were conducted at room temperature using a constant vertical displacement velocity of 4.94±0.04 mm/min. The thickness, width, and length of neat and reinforced TPS sheets were measured by using a digital micrometer with an accuracy of ±1 μm (Mitutoyo) and a caliper with an accuracy of ±30 μm (Control Company). As stated in the ASTM D638-22 test method, specimens were conditioned in desiccators with silica gel at 25±1 °C and a relative humidity (RH) of 50% for five days before the test. Temperature and percentage of RH inside desiccators were recorded using digital hygrometers (Sper Scientific) with a resolution of ±0.1 °C and 1% RH, respectively. The tensile stress, σ, and uniaxial strain, ε, were calculated as follows:

$$\sigma = \frac{F}{A} \tag{1}$$

$$\varepsilon = \frac{\Delta l}{l_0} \tag{2}$$

where F is the normal force applied on a surface A, $\Delta l = l - l_0$ is the uniaxial elongation, and l and l_0 are the instantaneous and initial lengths of the specimen, respectively. The reported values of σ and ε for neat and reinforced TPS sheets were the average of twelve measurements, always using fresh samples.

2.2.3 *Water vapor transmission*

Barrier property evaluation of TPS/AFs was performed according to the ASTM E96/E96M-22a test method, calculating the water vapor permeability as the product of water vapor permeance (WVP) and thickness of samples. It is well known that the thickness of the sample influences water vapor permeability (Bertuzzi *et al*., 2007). Therefore, the WVP was calculated since it is only affected by the water vapor mass flow that occurs perpendicularly to the surface of the specimen, A_p, when separating two regions with specific humidity conditions. In this way, WVP was determined as follows:

$$WVP = \frac{G/t}{A_p(R_1 - R_2)} \tag{3}$$

where S is the saturated vapor pressure at the test temperature, R_1 and R_2 are the relative humidity in the desiccator and inside the test cell, respectively. G is the mass gain of the permeability cells due to the water vapor transmission as a function of time, t. In Equation (3), the factor $(G/t)/A_p$ is known as water vapor flux, and G/t is the slope (mass flow rate of water vapor) of the graph G *vs* t in the steady-state regime.

WVP tests were conducted by cutting four circular specimens of neat and reinforced TPS sheets of 0.033 m in diameter, whose thicknesses were measured with the digital caliper. Before the test, samples were conditioned for five days at 25±1 °C and 57±1% RH using a saturated NaBr solution as stated in the ASTM E104-20a test method. Temperature and RH inside desiccators were recorded using digital hygrometers. WVP aluminum cells were filled with standard $CaCl_2$ desiccant to ensure a 0% RH. The WVP cells were covered with the specimen and closed with an aluminum annulus tap. Once the cells were assembled, they were placed inside a desiccator with

a saturated KNO_3 aqueous solution to reach 93±2% RH at 25±1 °C. The values of *G* for each cell were recorded as a function of time until *G/t* was constant, i.e., until the water vapor transmission was steady. The mass of cells was determined by using an analytical balance with an accuracy of ±0.1 mg (Oertling, NA164). On the other hand, the aluminum cell, $CaCl_2$ desiccant, and samples of TPS sheets were weighed at the beginning and end of the test.

2.2.4 *Water solubility*

Water solubility (WS) of neat and reinforced TPS sheets is defined as the dried matter that solubilizes when the sample is immersed in water for a specific time (Escobar *et al*., 2009). WS test of neat and reinforced TPS sheets was conducted following the methodology proposed by López *et al*. (2008). Specimens of 0.02 m x 0.02 m of neat and reinforced TPS sheets were cut and conditioned at 25±1 °C for five days at 0% RH in a desiccator with silica gel. The initial mass ($W_{initial}$) of the dried specimens was recorded. The dried samples were placed in a beaker with 60 mL of bi-distilled water, keeping constant agitation for 1 hour at room temperature, and then all the content was filtered with a pre-weighted filter paper (grade 4, Whatman®). The filter paper with solids was dried in a convection oven at 60±0.4 °C for 2 hours (HERAtherm, ThermoScientific), and the final dried mass was obtained (W_{final}) by subtracting the mass of the filter paper. This procedure was conducted three times for each fiber concentration. Finally, the percentage of solubility was calculated as follows:

$$\%Sol = \frac{W_{initial} - W_{final}}{W_{initial}} \times 100 \qquad (4)$$

2.2.5 *Biodegradability*

The biodegradability of neat and reinforced TPS sheets was determined by following the ASTM D5988-18 test for determining the aerobic biodegradation of plastic materials in soil. The original test method follows the evolution of CO_2 to determine biodegradation in soil or compost as substrate. However, in this work, a photographic record was carried out to evaluate qualitatively the biodegradability of the TPS sheets. The soil, consisting of worm humus free of rocky material greater than 2 mm, was characterized to determine the parameters for the biodegradation test as pH, relative humidity, ashes, organic carbon, total Kjeldahl nitrogen, as well as the carbon-nitrogen (C/N) ratio according to the standard NMX-FF-109-SCFI-2008. All chemicals used for the proximate analysis of soil and TPS sheets were ACS reagent grade. The properties of soil are reported in Table 2.

The biodegradability tests were conducted using desiccators with 350 g of worm humus with a low nitrogen content of less than 2% and a microbial content greater than $8x10^6$ CFU per gram of wet matter. Before the test, samples of neat and reinforced (8 wt.% of AFs) TPS sheets were characterized to obtain the ashes, organic matter, and organic carbon, as shown in Table 2. The sheets of approximately 11.5 mm x 50 mm in size were placed on the worm humus in each desiccator. The initial mass of all samples was adjusted to 1.13±0.09 g, while thicknesses for neat and reinforced TPS sheets were 0.6±0.03 and 0.87±0.05 mm, respectively. A beaker with 50 mL of distilled water was placed on the perforated dish of each desiccator to ensure 99% RH. The desiccators were then sealed, and digital hygrometers were used to measure the temperature and relative humidity. The desiccators were opened for 30 minutes every 48 hours to allow aeration until the end of the test, which lasted 112 days. During this time, images were captured with a 16-megapixel CMOS camera (FinePix HS20EXR, Fuji Film) to record the biodegradation process of the TPS sheets. In addition, SEM images of TPS sheets were obtained using the EVO® LS10 microscope, which was used to qualitatively evaluate the physical integrity of samples due to biodegradation.

Table 2. Proximate composition analysis of model soil (worm humus), neat (0 wt.%), and reinforced (8 wt.%) TPS sheets with AFs.

Parameter	Model soil (worm humus)	Fiber content in TPS sheets (wt.%)	
		0	8
pH	8.15±0.2	--	--
Relative humidity (% RH)	37.37±2	--	--
Ashes (%)	54.02±0.03	0.14±0.03	0.36±0.05
Organic matter (%)	45.98±0.03	99.86±0.03	99.64±0.05
Organic carbon (%)	26.67±0.02	57.92±0.02	57.8±0.03
Kjeldahl total nitrogen (%NTK)	1.12	--	--
C/N ratio	23.8	--	--

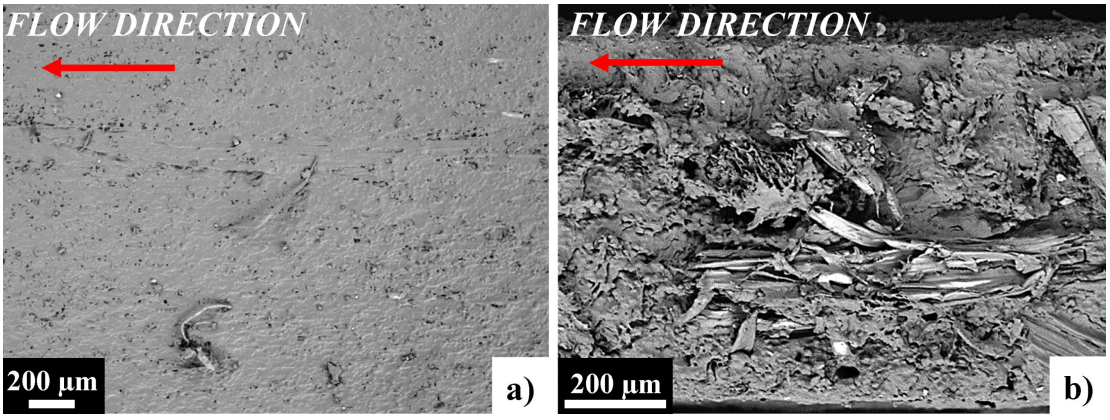

Figure 2. SEM images of reinforced TPS sheets with 8 wt.% of AFs of the (a) surface and (b) the longitudinal cross section of sheets after processing. Red arrows indicate flow (extrusion) direction.

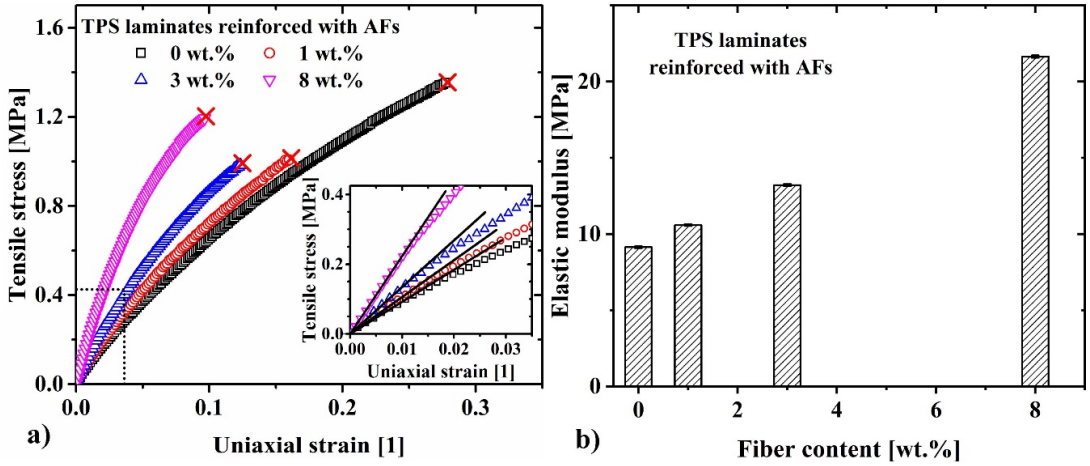

Figure 3. (a) Tensile stress curves as a function of the uniaxial strain for the neat and reinforced TPS sheets with different AFs contents. The reported curves are the average of twelve measurements. The red crosses indicate the ultimate tensile stress and the strain at break. Solid lines in the inset indicate the data fittings to a linear model used to obtain the elastic modulus, plotted in (b) as a function of AFs concentration.

3 Results and discussions

3.1 The physical appearance of TPS sheets

The neat TPS sheets showed a uniform appearance on their surface. In the case of the reinforced sheets, SEM images reveal that fibers are well distributed in the TPS matrix with roughness increasing along with the AFs content (see Figure 2). Specifically, Figure 2a shows a SEM image of the surface of a TPS sheet with 8 wt.% of AFs, while Figure 2b depicts its longitudinal cross section. On the other hand, polarized light microscopy of the TPS sheets (not presented here) revealed some granules showing the Maltese cross pattern (as in Figure 1b), indicating an incomplete fusion process. However, some authors have indicated that this pattern may be attributed to residual crystallinity and rapid retrogradation induced by processing (van Soest *et al*., 1996, 1997; Bertoft, 2017; Cornejo-Ramírez et al., 2018).

It should be noted that TPS sheets reinforced with different contents of AFs possess surface morphology that makes them a good candidate for eco-friendly packaging and as a substitute for single-use plastics. These applications will be possible if they exhibit suitable physicochemical properties such as proper mechanical resistance for the manufacturing process and water vapor barrier properties, and mainly, they must degrade or preferably be biodegradable to reduce their impact on the environment at the end of their useful life. In the following sections we evaluate the mechanical and barrier properties of the TPS sheets reinforced with different contents of AFs.

Table 3. Values of UTS (indicated with a red cross mark in Figure 3a), strain at break, and elastic modulus of neat and reinforced TPS sheets.

	Biocomposites with AFs content (wt.%)			
	0	1	3	8
UTS (MPa)	1.36±0.13	1.02±0.08	0.99±0.04	1.2±0.09
SB (1)	0.28±0.04	0.16±0.02	0.13±0.01	0.1±0.01
Elastic modulus, E (MPa)	9.14±0.07	10.59±0.07	13.1±0.08	21.64±0.09
Resilience (kJ/m^3)	0.89±0.05	1.09±0.06	1.4±0.09	2.34±0.12
Tenacity (kJ/m^3)	221.75±4.79	94.73±5.15	73.18±3.27	71.99±4.61

3.2 Tensile properties of TPS sheets

The tensile stress curves as a function of the uniaxial strain for both neat and reinforced TPS sheets with different contents of AFs are shown in Figure 3a. The average values of the ultimate tensile stress (UTS) and uniaxial strain at break (SB) for each biocomposite are represented by the red crosses at the end of each deformation curve (refer to Table 3 for details). The results in Figure 3 and Table 3 indicate that neat TPS sheets have higher UTS and SB values compared to reinforced TPS with AFs. The UTS value reaches a minimum between 1 and 3 wt.% of AFs, likely due to micro-cracks formation caused by the fibers that are not oriented in the direction of flow. However, once the fiber concentration rises from 3 to 8 wt.%, the UTS increases, which can be attributed to the fiber orientation caused by mechanical interactions during processing (Ku *et al*., 2011; Ji *et al*., 2021; Józó et al., 2022; Majeed *et al*., 2013).

On the other hand, in Figure 3a, it was possible to find a region fitted by a linear-elastic solid model at low uniaxial strain marked by dotted lines. The upper limit of the linear region was identified as the last point located within a 2% band defined by the difference between the experimental stress and that obtained with the linear model (see inset in Figure 3a). The slope of the linear region, which is the modulus of Young or elastic modulus E, is presented in Figure 3b as a function of AFs concentration. The value of E increases linearly with the fiber content up to 3 wt.% AFs in semiconcentrated regime and nonlinearly for higher concentrations of AFs, as expected for concentrated composites (Maya *et al*., 2008). The increase of E indicates that the reinforced TPS sheets are stiffer than the control (0% of AFs); also, the obtained values are comparable in magnitude to those found in the literature for nanoclays used as reinforcement (Ku *et al*., 2011; Ji *et al*., 2021; Józó *et al*., 2022; Majeed *et al*., 2013; Mohanty *et al*., 2018). However, the E values are still lower than those obtained for synthetic polymers (Mark, 1999). Another factor that influences the UTS values of reinforced TPS sheets is the difference in the tensile strength between fibers and the TPS matrix. To explore this issue, TPS sheets with 8 wt.% AFs were analyzed after breakage in the tensile test. SEM micrographs in Figure 4 reveal bared, non-saggy, and unbroken fibers in the breaking section of sheets. This may be due to the difference in tensile strength of fibers and the TPS matrix, as the tensile strength values for AFs are between 20-290 MPa, while that of neat TPS is around 1.18 MPa (Biagiotti *et al*., 2004; Mohanty *et al*., 2018). This indicates that AFs possess a lower deformation capability than the matrix, which could result in a decrease in the SB, as observed in Figure 3a. In addition, SEM micrographs also evince that superficial forces between matrix and fibers are weak (see the naked fibers in the middle and right parts of Figure 4), and the use of proper additives during the blending process could help to increase matrix-fiber interactions and make TPS sheets stronger. Nevertheless, this is beyond the scope of this work and needs further investigation.

Manufacturing casings for packaging requires materials with high resilience and tenacity so that the final products can withstand loads without deforming or breaking. Table 3 shows the resilience and tenacity values of the neat and reinforced TPS sheets. It was observed that resilience increases along with the fiber content, as expected, due to the presence of the AFs that contribute to an increase in stiffness of the reinforced TPS sheets, with the fact that $E_{AFs}>E_{TPS}$. At the same time, the tenacity of reinforced TPS sheets decreases as the concentration of AFs increases, which is also associated with the increment of their stiffness that restricts plastic deformation. These findings suggest that reinforced TPS sheets could be a viable alternative to packaging and single-use plastics that contain AFs.

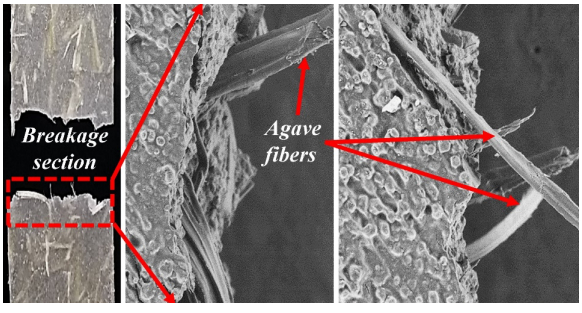

Figure 4. SEM micrographs of the breakage section of TPS sheets with 8 wt.% of AFs.

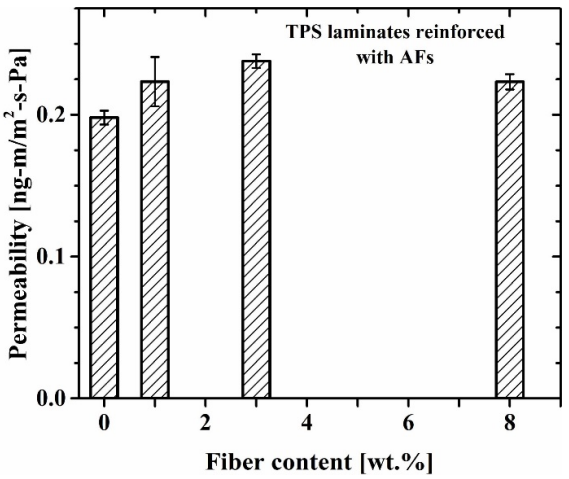

Figure 5. Water vapor permeability of TPS sheets as a function of AFs concentration.

3.3 Barrier properties and water solubility

The water vapor permeability of TPS sheets as a function of AFs concentration is shown in Figure 5. There is a maximum at 3 wt.% of AFs, indicating that water vapor is diffusing quickly at low concentration of AFs (≤3 wt.%), whereas, at 8 wt.%, it diffuses slowly throughout the composite, reducing the mass flow rate passing through the sheet of given thickness and cross-sectional area. It is expected that permeability will decrease as the fiber content increases. However, the mass flow rate reduction may be attributed to the variation in the specimen thickness, which is difficult to control during processing and affects the water vapor permeability (Bertuzzi *et al*., 2007; Kim *et al*., 2015).

In Figure 6a, the WVP of reinforced TPS sheets is plotted as a function of AFs content in the TPS matrix, where it is observed that WVP decreases as the concentration of AFs in the TPS matrix increases. This observation helps in eliminating the effect of thickness on water permeability. In fact, WVP of TPS sheets reinforced with 3 and 8 wt.% of AFs reduces approximately 14 and 29% compared to neat sheets, respectively, which indicates that the water vapor barrier property of TPS biocomposites is improved by adding AFs. No significant changes in WVP were observed for 1 wt.% of AFs in the TPS sheets.

To elucidate the mass transfer mechanism, the initial and final weights of the $CaCl_2$ desiccant, sheets, and aluminum cell were recorded to calculate the mass gain of desiccant, *G*, plotted as a function of the AFs concentration in Figure 6b. As the concentration of AFs increases, fibers get closer to each other, and *G* decreases; this indicates that water vapor diffuses more slowly towards the desiccant, reducing WVP. The negative value of *G* observed for the TPS sheets can be interpreted as a loss of mass. This is due to the fact that fibers restrict WVP, and the drying of reinforced TPS sheets takes place instead. This explanation has been handled in different works as a tortuous path followed by vapor water (Majeed *et al*., 2013).

Regarding the solubility of TPS sheets in water as a function of fiber content, a decrease of 17% was calculated with the incorporation of 8 wt.% of AFs compared to the TPS matrix. Note that the capability of TPS sheets to dissolve is due to the interaction of water with the hydroxyl groups of the starch components (amylose), which causes the dissociation of the matrix and its solubilization in water (Kim *et al*., 2015). As the content of AFs in the TPS matrix increases, the solubility decreases due to the presence of components such as cellulose, hemicellulose, and lignin that are insoluble in water (Majeed et al., 2013; Maya *et al*., 2008). Therefore, TPS sheets are beneficial for producing films, sheets, or profiles that can be used as packaging or single-use bioplastics (García-Guzman *et al*., 2022; Jiang *et al*., 2020). This can help in replacing synthetic plastics.

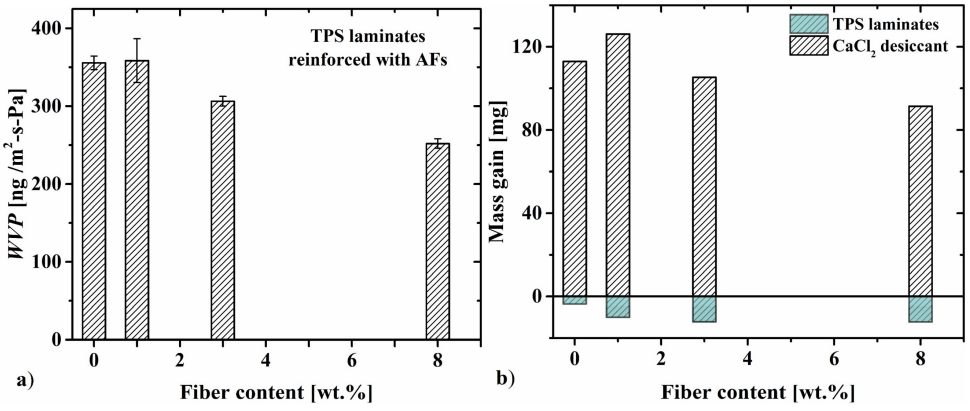

Figure 6. (a) Water vapor permeance of TPS sheets and (b) mass gains of $CaCl_2$ desiccant and TPS sheets as a function of AFs concentration.

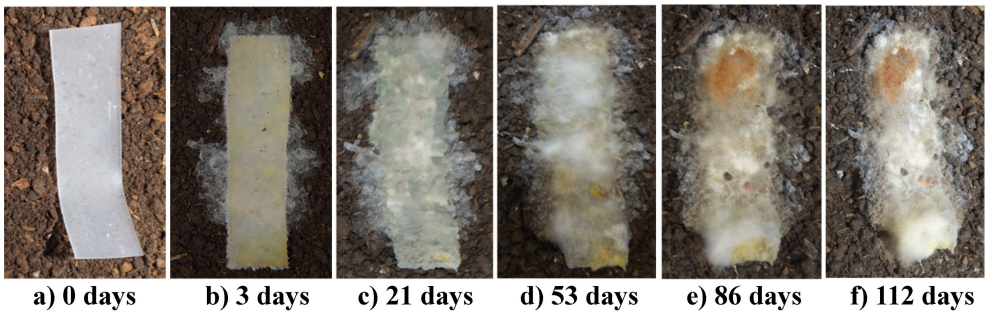

Figure 7. Photographic record of neat TPS sheet degradation in a model soil (worm humus) from 0 to 112 days of the test.

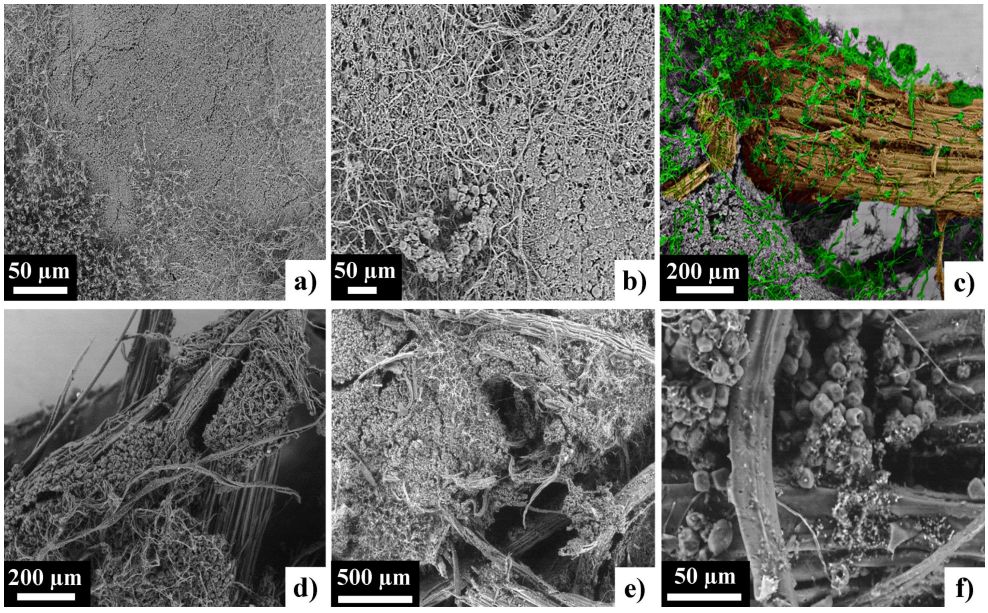

Figure 8. SEM micrographs of the surface of biodegraded neat and reinforced (8 wt.% of AFs) TPS sheets (a and b) after 21 days from the start of the test. Images (c)-(f) correspond to the reinforced TPS sheet after 28 days. The colors in the image (c) indicate the starch matrix (gray), AFs (brown), and mycelium (green).

3.4 Biodegradability

The susceptibility of TPS sheets to be biodegraded by bacteria and/or fungi was investigated following the ASTM D5988-18 test method, which establishes the procedure to quantify the CO_2 produced by the biodegradation of the organic matter present in the biocomposites. The tests carried out following this method allowed us to conclude that it is necessary to strictly control parameters such as the specific characteristics of the soil, as well as the type and quantity of microorganisms per unit mass of soil and specimen. The control of the latter and the mechanism for capturing and quantifying the gases produced (CO_2, CH_4, etc.) from the biodegradation of the specimen are not established in the standard. For these reasons, the photographic record of the biodegradation process was only carried out under the conditions stated in the standard since visual changes such as surface roughness, formation of holes or cracks, or differences in coloration can indicate some microbial attack (Ahmed *et al*., 2018; Ali *et al*., 2008; García-Guzman *et al*., 2022; Idris *et al*., 2023; Jiang *et al*., 2020; Rosa *et al*., 2009; Samir *et al*., 2022; Surendren *et al*., 2022).

Figure 7 shows the photographic evidence of TPS sheets that were tested for biodegradability. After three days, fungi growth occurred on the surface of the sheet. As time passed, bacterial and fungal proliferation increased, as seen in the same figure at day 21, a proof that the sheet was being biodegraded by the action of the bacterial and/or fungal consortia. After 112 days of exposure to controlled conditions, the dimensions of the sheets decreased and the specimens lost their physical integrity, ultimately leading to their breakage.

On the other hand, Figure 8 shows the environmental SEM micrographs of the surface of neat and reinforced (8 wt.% of AFs) TPS sheets. In Figures 8a and 8b, the surface of neat and reinforced TPS sheets, respectively, display the growth of mycelium

and proliferation of a fungus (not identified in this work) after 21 days of testing. This indicates that TPS sheets are undergoing biodegradation, which is appreciated by the loss of physical integrity and the appearance of cracks on their surface. This stage is known as the start of fragmentation (Rosa *et al*., 2009; Ahmed *et al*., 2018; Idris *et al*., 2023).

Figures 8c and 8d depict micrographs of the reinforced TPS sheets 28 days after the start of the test in different sectors of the sheet. During this stage, fungi spread on the surface of sheets, and fibers were partially exposed from the matrix, which was also attacked by fungi and bacteria (mycelium is colored green). Furthermore, cracks on the surface of sheets became more extensive than those from the previous stage, causing a lack of physical integrity. These findings suggest that the second stage of biodegradation, called deterioration, has begun (Ahmed *et al*., 2018; Ali *et al*., 2008; Idris *et al*., 2023). Figures 8e and 8f demonstrate the deterioration of sheets caused by the matrix degradation. The matrix is more susceptible to biodegradation than AFs, which are known to require a longer time to achieve biodegradation due to their high cellulose content. Figure 8f shows starch granules separated from the matrix, which can be associated with sheet deterioration before the assimilation stage. It is important to mention that the physical condition of the sheets at the assimilation stage is similar to those shown in Figures 8e and 8f. It was impossible to obtain SEM images of sheets in this stage because the sheets disintegrated during their removal from the soil.

The micrographs presented in Figures 7 and 8 show that the initial attack of microorganisms occurs on the surface of sheets. This process leads to a change in the physicochemical properties of the biocomposites, i.e., bacteria and fungi adhere to and colonize the sheet surface to reduce the strength and durability of the neat and reinforced TPS sheets (Figures 7a-b and Figures 8a-b). Then, during the deterioration stage, the surface of TPS sheets displays cracks caused by the enzymatic activity of intracellular or extracellular microbial enzymes, mainly amylose (Idris *et al*., 2023). This process is followed by fragmentation, which results in a decrease in the molecular weight of the biopolymer chains (mainly amylose) and oxidative degradation of the lower molecular weight molecules. The micrographs in Figures 8d-f show that the fibers remain intact or less degraded than the TPS matrix. This is because microorganisms cannot break down the cellulose chains. On day 28, microorganisms attacked the amorphous areas, where the biopolymer chain molecular weight was reduced by enzymatic activity. However, the crystalline regions (amylopectin chains) were less degraded, in agreement with that reported by different authors (Ahmed *et al*., 2018; Idris *et al*., 2023; Rosa *et al*., 2009; Samir *et al*., 2022; Surendren *et al*., 2022).

The third stage of the biodegradation process is assimilation. In this stage, the low molecular weight molecules, which were created in the fragmentation phase, serve as a source of carbon and energy for microorganisms to grow and respirate (see Figures 8e and f). The last stage is mineralization, where carbon dioxide, water, or methane may be produced after degradation (see Figure 8f). To close this section, it may be said that the identification of the microorganisms contained in the soil and those that participated in the biodegradation of the sheets was not carried out; however, those that degrade starch are known to include *Aspergillus niger*, *Penicillium funiculosum*, *Phanerochaete chrysosporium*, and *Streptomyces* (Ahmed *et al*., 2018; Ali *et al*., 2008; Idris *et al*., 2023; Jiménez-Pérez *et al*., 2023).

Finally, it was shown that AF fibers in the TPS matrix did not modify the biodegradability of the biocomposites, only a delay of a few days in the biodegradation process of the reinforced TPS sheets was observed since cellulose fibers are less susceptible to being biodegraded than starch. This work shows that the mechanical and barrier properties of biodegradable TPS sheets reinforced with AF fibers obtained by extrusion were significantly improved. These results suggest that reinforced TPS sheets can be an alternative to packaging and single-use plastics to fulfill the current international policies (Filiciotto *et al*., 2021).

Conclusion

Thermoplastic corn starch/*Agave tequilana* fiber biocomposites obtained by continuous extrusion exhibit mechanical and physicochemical properties suitable for producing biodegradable materials that can help to replace packaging polymers and single-use synthetic plastics. TPS biocomposite sheets exhibit a flat surface and become rougher as the fiber content increases. Regarding the mechanical properties of biocomposites, the ultimate tensile stress and uniaxial deformation decrease with the addition of fibers. Adding AFs at 8 wt.% to TPS sheets leads to a significant increase (136%) in their elastic modulus. However, as the concentration of AFs increases, the tenacity of both neat and reinforced TPS sheets decreases due to the increase in stiffness of reinforced TPS. On the other hand, the biocomposite sheets exhibit an improvement in resilience as the fiber content increases, which is a desirable attribute for manufacturing casings for packaging. Concerning barrier properties, the reinforced TPS sheets display a 29% reduction in water permeance when 8 wt.% of AFs is incorporated. Additionally, the water

solubility of the sheets decreases by up to 17%. These changes can be attributed to the difference in the hydrophobic/hydrophilic characteristics of the fibers and the matrix. From this, it is essential to consider the interactions between the components of the biocomposites and the appropriate amount of reinforcement required to achieve the desired barrier properties for specific applications. Moreover, TPS sheets, both neat and reinforced, are susceptible to biodegradation by bacteria and fungi consortia in soil. Photographic records show that sheets lose their physical integrity over time due to the biodegradation of starch (matrix). Furthermore, the more amorphous the starch matrix is, the faster it biodegrades.

Nomenclature

TPS	Thermoplastic starch
UTS	Ultimate tensile stress
SB	Strain at break
AFs	*Agave tequilana* fibers
WS	Water solubility
SEM	Scanning electron microscopy
ASTM	American Society for Testing and Materials
USP	United States Pharmacopeia
D_w	Average-weight diameter of fibers
L_w	Average-weight length of fibers
r_w	Average-weight aspect ratio of fibers
φ	Concentration of *Agave tequilana* fibers
F	Normal force applied on a surface
A	Surface over the force F is applied
l_0	Original length of the test specimen
l	Instantaneous length of the test specimen
σ	Tensile stress
ε	Uniaxial strain
E	Modulus of Young or elasticity
WVP	Water vapor permeance
G	Mass gain of the permeability cells
t	Time
A_p	Cross section of the specimen in the permeability test
R_1	Relative humidity in the desiccator
R_2	Relative humidity inside the permeability test cell
$CaCl_2$	Calcium chloride
NaBr	Sodium bromide
KNO_3	Potassium nitrate
$W_{initial}$	Initial mass of dried specimen
W_{final}	Final mass of the dried specimen after the test
$\%Sol$	Water solubility percentage of the specimen

References

Ahmed, T., Shahid, M., Azeem, F., Rasul, I., Ali Shah, A., Noman, M., Hameed, A., Manzoor, N., Manzoor, I. and Muhammad, S. (2018). Biodegradation of plastics: current scenario and future prospects for environmental safety. *Environmental Science and Pollution Research*, *25*, 7287-7298. https://doi.org/10.1007/s11356-018-1234-9.

Alanís-López, P., Pérez-González, J., Rendón-Villalobos, R., Jiménez-Pérez, A., and Solorza-Feria, J. (2011). Extrusion and Characterization of Thermoplastic Starch Sheets from "Macho" Banana. *Journal of Food Science*, *76*(6), E465-E471. https://doi.org/10.1111/j.1750-3841.2011.02254.x.

Ali, S.A., Fariha, H., Abdul, H., and Safia, A.

Acknowledgements

This research was supported by SIP-IPN (20230817, 20240661, 20240882). E. F. M.-B. is a recipient of a CONAHCYT postdoctoral fellowship. Special thanks to Prof. José Pérez-González for providing the infrastructure of the Laboratorio de Reología y Física de la Materia Blanda to carry out part of this work.

(2008). Biological degradation of plastics: A comprehensive review. *Biotechnology Advances*, *26*(3), 246-265. https://doi.org/10.1016/j.biotechadv.2007.12.005.

Aranda-García, F.J., González-Núñez, R., Jasso-Gastinel, C.F., and Mendizábal, E. (2015). Water Absorption and Thermomechanical Characterization of Extruded Starch/Poly(lactic acid)/Agave Bagasse Fiber Bioplastic Composites. *International Journal of Polymer Science*, *2015*, 343294. https://doi.org/10.1155/2015/343294.

Bertoft, E. (2017). Understanding Starch Structure: Recent Progress. *Agronomy*, *7*(3), 56; https://doi.org/10.3390/agronomy7030056.

Bertuzzi, M.A., Castro Vidaurre, E.F., Armada, M., and Gottifredi, J.C. (2007). Water vapor permeability of edible starch based films. *Journal of Food Engineering*, *80*(3), 972-978. https://doi.org/10.1016/j.jfoodeng.2006.07.016.

Biagiotti, J., Puglia, D., and Kenny, J.M. (2004). A Review on Natural Fibre-Based Composites-Part I: Structure, Processing and Properties of Vegetable Fibres. *Journal of Natural Fibers*, *1*(2), 37-68. https://doi.org/10.1300/J395v01n02_04.

Castro-Montoya, Y.A., Jacobo-Valenzuela, N., Delgad-Nieblas, C.I., Ruiz-Armenta, X.A., Heredia, J.B., Delgado-Murillo, S.A., Calderon-Castro, A., and Zazueta-Morales, J.J. (2024). Effect of the extrusion process on phytochemical, antioxidant, and cooking properties of gluten-free pasta made from broken rice and nopal. *Revista Mexicana de Ingeniería Química*, *23*(1), Alim24149, 1-15. https://doi.org/10.24275/rmiq/Alim24149.

Cheng, H., Chen, L., McClements D.J., Yang, T., Zhang, Z., Ren., F., Mao, M., Tian, Y., and Jin, Z. (2021). Starch-based biodegradable packaging materials: A review of their preparation, characterization and diverse applications in the food industry. *Trends in Food Science and Technology*, *114*, 70-82. https://doi.org/10.1016/j.tifs.2021.05.017.

Cornejo-Ramírez, Y.I., Martínez-Cruz, O., Del Toro-Sánchez, C.L., Wong-Corral, F.J., Borboa-Flores, J., and Cinco-Moroyoqui, F.J. (2018). The structural characteristics of starches and their functional properties, *CyTA - Journal of Food*, *16*(1), 1003-1017. https://doi.org/10.1080/19476337.2018.1518343.

do Val Siqueira, L., La Fuente Arias, K.I., Chieregato Maniglia, B., and Tadini C. C. (2021). Starch-based biodegradable plastics: methods of production, challenges and future perspectives. *Current Opinion in Food Science*, *38*, 122-130. https://doi.org/10.1016/j.cofs.2020.10.020.

dos Reis, R.C., Devilla, I.A., Oliveira, G.H.H., Côrrea, P. C., Ascheri, D. P. R., Souza, A.B.M., and Servulo, A.C.O. (2014). Mechanical properties, permeability and solubility of films composed of yam starch and glycerol. *Interciencia: Revista de ciencia y tecnología de América*, *39*(6), 410-415. https://www.interciencia.net/wp-content/uploads/2017/11/410-c-DOS-REIS-6.pdf.

Escobar, D., Sala, A., Silvera, C., Harsipe, R., and Márquez, R. (2009). Películas biodegradables y comestibles desarrolladas en base a aislado de proteínas de suero lácteo: estudio de dos métodos de elaboración y del uso de sorbato de potasio como conservador. *INNOTEC*, *4*, 33-36. https://doi.org/10.26461/04.07.

Filiciotto, L., and Rothenberg, G. (2021). Biodegradable plastics: Standards, policies, and Impacts. *ChemSusChem*, *14*(1), 56-72. https://doi.org/10.1002/cssc.202002044.

Fitch-Vargas, P.R., Camacho-Hernández, I.L., Rodríguez-González, F.J., Martínez-Bustos, F., Calderón-Castro, A., Zazueta-Morales, J. de J., and Aguilar-Palazuelos E. (2023). Effect of compounding and plastic processing methods on the development of bioplastics based on acetylated starch reinforced with sugarcane bagasse cellulose fibers. *Industrial Crops and Products*, *192*, 116084. https://doi.org/10.1016/j.indcrop.2022.116084.

Folino, A., Karageorgiou, A., Calabrò, P. S., and Komilis, D. (2020). Biodegradation of Wasted Bioplastics in Natural and Industrial Environments: A Review. *Sustainability*, *12*(15), 6030; https://doi.org/10.3390/su12156030.

García-Guzmán, L., Cabrera-Barjas, G., Soria-Hernández, C. G., Castaño, J., Guadarrama-Lezama, A.Y., and Rodríguez Llamazares, S. (2022). Progress in Starch-Based Materials for Food Packaging Applications. *Polysaccharides*, *3*(1), 136-177. https://doi.org/10.3390/polysaccharides3010007.

Idris, S.N., Amelia, T.S.M., Bhubalan, K., Lazim, A.M.M., Ahmad, N.A.M., Jamaluddin, Z.M.I., Santhanam, R., Amirul, A.-A.A.,

Vigneswari, S., and Ramakrishna, S. (2023). The degradation of single-use plastics and commercially viable bioplastics in the environment: A review. Environmental Research, 231(1), 115988. https://doi.org/10.1016/j.envres.2023.115988.

Ji, M., Li, F., Li, J., Li, J., Zhangc, C., Sun, K., and Guoa, Z. (2021). Enhanced mechanical properties, water resistance, thermal stability, and biodegradation of the starch-sisal fibre composites with various fillers. *Materials and Design*, *198*, 109373. https://doi.org/10.1016/j.matdes.2020.109373.

Jiang, T., Duan, Q., Zhu, J., Liu, H., and Yu, L. (2020). Starch-based biodegradable materials: Challenges and opportunities. *Advanced Industrial and Engineering Polymer Research*, *3*, 8-18. https://doi.org/10.1016/j.aiepr.2019.11.003.

Jiménez-Pérez, C., Gómez-Ruiz, L., González-Olivares, L. G., Fernández, F. J., and Cruz-Guerrero, A. E. (2023). Biodegradation of polystyrene with laccase-producing enterobacteria isolated from a municipal waste dump. *Revista Mexicana de Ingeniería Química*, *22*(1), Bio2971, 1-8. https://doi.org/10.24275/rmiq/Bio2971.

Józó, M., Várdai, R., Bartos, A., Móczó, J., and Pukánszky, B. (2022). Preparation of Biocomposites with Natural Reinforcements: The Effect of Native Starch and Sugarcane Bagasse Fibers. *Molecules*, *27*(19), 6423. https://doi.org/10.3390/molecules27196423.

Kim, S.R.B., Choi, Y.-G., Kim, J.-Y., and Lim, S.-T. (2015). Improvement of water solubility and humidity stability of tapioca starch film by incorporating various gums. *LWT - Food Science and Technology*, *64*(1), 475-482. https://doi.org/10.1016/j.lwt.2015.05.009.

Ku, H., Wang, H., Pattarachaiyakoop, N., and Trada, M. (2011). A review on the tensile properties of natural fiber reinforced polymer composites. *Composites Part B: Engineering*, *42*(4), 856-873. https://doi.org/10.1016/j.compositesb.2011.01.010.

López, M.G., Mancilla-Margalli, N.A., and Mendoza-Diaz, G. (2003). Molecular Structures of Fructans from Agave tequilana Weber var. Azul. *J. Agric. Food Chem.*, *51*(27), 7835-7840. https://doi.org/10.1021/jf030383v.

López, O.V., García, M.A., and Zaritzky, N.E. (2008). Film forming capacity of chemically modified corn starches. *Carbohydrate Polymers*, *73*(4), 573-581. https://doi.org/10.1016/j.carbpol.2007.12.023.

Majeed, K., Jawaid, M., Hassan, A., Abu Bakar, A., Abdul Khalil, H.P.S., Salema, A.A., and Inuwa, I. (2013). Potential materials for food packaging from nanoclay/natural fibres filled hybrid composites. *Materials and Design*, *46*, 391-410. https://doi.org/10.1016/j.matdes.2012.10.044.

Mark, J. E. (1999). *Polymer Data Handbook*. Oxford University Press, USA.

Maya, J.J., and Sabu, T. (2008). Biofibres and biocomposites. *Carbohydrate Polymers*, *71*, 343-364. https://doi.org/10.1016/j.carbpol.2007.05.040.

Mohanty, A.K., Vivekanandhan, S., Pin, J.-M., and Misra, M. (2018). Composites from renewable and sustainable resources: Challenges and innovations. *Science*, *362*(1), 536-542. https://doi.org/10.1126/science.aat9072.

Rosa, M.F., Chiou, B.-S., Medeiros, E.S., Wood, D.F., Mattoso, H.C., Orts, W.J., and Imam, S.H. (2009). Biodegradable Composites Based on Starch/EVOH/Glycerol Blends and Coconut Fibers. *Journal of Applied Polymer Science*, *111*, 612-618. https://doi.org/10.1002/app.29062.

Samir, A., Ashour, F.H., Abdel Hakim, A.A., and Bassyouni, M. (2022). Recent advances in biodegradable polymers for sustainable applications. *NPJ Materials Degradation*, *6*, 68. https://doi.org/10.1038/s41529-022-00277-7.

Surendren, A., Mohanty, A.K., Liu, Q., and Misra, M. (2022). A review of biodegradable thermoplastic starches, their blends and composites: recent developments and opportunities for single-use plastic packaging alternatives. *Green Chem.*, *24*, 8606-8636. https://doi.org/10.1039/D2GC02169B.

Tabasum, S., Younas, M., Zaeem, M.A., Majeed, I., Majeed, M., Noreen, A., Iqbal, M.N., and Zia, K.M. (2019). A review on blending of corn starch with natural and synthetic polymers, and inorganic nanoparticles with mathematical modeling. *International Journal of Biological Macromolecules*, 122, 969-996. https://doi.org/10.1016/j.ijbiomac.2018.10.092.

van Soest, J.J.G., Hulleman, S.H., de Wit, D., and Vliegenthart, J.F.G. (1996). Crystallinity in starch bioplastics. *Industrial Crops and Products*, *5*(1), 11-22. https://doi.org/10.1016/0926-6690(95)00048-8.

van Soest, J.J.G., and Knooren, N. (1997). Influence of glycerol and water content on the structure and properties of extruded starch plastic sheets during aging. *Journal of Applied Polymer Science*, *64*(7), 1411-1422. https://doi.org/10.1002/(SICI)1097-4628(19970516)64:7%3c1411::AID-APP21%3e3.0.CO;2-Y.

Wazeer, A., Das, A., Abeykoon, C., Sinha, A., and Karmakar, A. (2023). Composites for electric vehicles and automotive sector: A review. *Green Energy and Intelligent Transportation*, *2*, 100043. https://doi.org/10.1016/j.geits.2022.100043.